



Dynamics of Continuous-Time Image Reconstruction System for Computed Tomography

Omar Abou Al-Ola[†], Ken'ichi Fujimoto[‡], and Tetsuya Yoshinaga[‡]

[†]Graduate School of Health Sciences, and [‡]Institute of Health Biosciences,
 The University of Tokushima, Tokushima 770-8509, Japan
 Email: {omar@x.fujimoto@|yosinaga@}medsci.tokushima-u.ac.jp

Abstract— This paper investigates dynamical properties of a continuous-time image reconstruction (CIR) system for computed tomography. We verify that an objective function of the inverse regularization problem decreases in time along the solutions to differential equations describing the CIR system. Moreover we illustrate that the system could reconstruct images with ensuring positive pixel values for simulated projection data.

1. Introduction

In this paper, we investigate a continuous-time image reconstruction (CIR) system [1, 2] described by differential equations. We have proposed the system for reconstructing tomographic medical images [3, 4] using its implementation in an analog electronic circuit, whose reconstruction speed is higher than that of software-based iterative methods [5, 6, 7, 8].

The CIR is a system of continuous dynamical methods [9, 10, 11, 12, 13, 14] for the regularization of ill-posed inverse problems [15] in computed tomography with noisy projection data. The conventional linear continuous method [16] produces negative values, which are physically impossible as a pixel image. The non-negativity constraint necessitates nonlinear continuous methods, including our CIR system.

We investigate that an objective function of the inverse regularization problem decreases in time along the solutions to differential equations describing the CIR system. Moreover we illustrate that the system could reconstruct images for simulated projection data.

2. CIR System

The basic problem of CT is to reconstruct an image using data acquired from projections [3, 4]. Our task is to obtain the pixel values $\mathbf{x} \in \mathbb{R}_+^J$, with \mathbb{R}_+ denoting the set of non-negative real numbers, satisfying

$$\mathbf{y} = \mathbf{A}\mathbf{x}, \quad (1)$$

where $\mathbf{y} \in \mathbb{R}_+^I \setminus \{\mathbf{0}\}$ is the projection value, and $\mathbf{A} \in \mathbb{R}_+^{I \times J} \setminus \{\mathbf{0}\}$ is a normalized projection operator. For

inconsistent projection data, Eq. (1) is an ill-posed problem, which means that its solution is not unique or does not exist [15]. Therefore, instead of solving Eq. (1), we consider the optimization problem

$$\begin{aligned} \min_{\mathbf{x}(t) \in \mathbb{R}_+^J} V(\mathbf{x}(t)), \quad t \in \mathbb{R}, \\ V(\mathbf{x}) := \frac{1}{2} \|\mathbf{y} - \mathbf{A}\mathbf{x}\|_2^2. \end{aligned} \quad (2)$$

To obtain a local minimum of the objective function, one can compute limit sets of evolutions of continuous dynamical systems [9, 10, 11, 13]. We have proposed [1, 2] a continuous dynamical method as an initial value problem in the following form

$$\begin{aligned} \frac{d\mathbf{x}}{dt} &= -\mathbf{X} \frac{\partial V}{\partial \mathbf{x}}(\mathbf{x})^\top \\ &= \mathbf{X}\mathbf{A}^\top (\mathbf{y} - \mathbf{A}\mathbf{x}), \quad (3) \\ t &\in \mathbb{R}_+, \quad \mathbf{x}(0) = \mathbf{x}_0, \end{aligned}$$

where $\mathbf{X} := \text{diag}(\mathbf{x})$ indicates the diagonal matrix of order $J \times J$ in which the corresponding diagonal elements are elements of \mathbf{x} .

3. Theoretical Result

The gradient system in Eq. (3) is a modification from the linear continuous system [16]

$$\begin{aligned} \frac{d\mathbf{x}}{dt} &= -\frac{\partial V}{\partial \mathbf{x}}(\mathbf{x})^\top \\ &= \mathbf{A}^\top (\mathbf{y} - \mathbf{A}\mathbf{x}), \quad (4) \\ t &\in \mathbb{R}_+, \quad \mathbf{x}(0) = \mathbf{x}_0, \end{aligned}$$

to enforce the positivity of its solutions. Let $\phi(t, \mathbf{x}_0)$ be a solution to Eq. (3) with initial value \mathbf{x}_0 , and \mathbb{R}_{++} denote the set of positive real numbers. The nonlinear system has the property that $V(\mathbf{x})$ decreases along the solution $\phi(t, \mathbf{x}_0)$ in time through the initial state $\mathbf{x}_0 \in \mathbb{R}_{++}^J$ at $t = 0$, which is supported by the following proposition.

Proposition 1. Consider Eq. (3) with $\mathbf{x}_0 \in \mathbb{R}_{++}^J$. If there exists a locally unique equilibrium $\mathbf{x}^* \notin \{\mathbf{0}\}$, then $V(\phi(t, \mathbf{x}_0))$ decreases in $t \in \mathbb{R}_+$.

Proof. We have $V(\mathbf{x}) \geq 0$ with equality if $\mathbf{x} = \mathbf{x}^* \notin \{\mathbf{0}\}$. Its derivative along the solution is given by

$$\frac{dV}{dt}(\phi(t, \mathbf{x}_0)) = -\mathbf{\Lambda}(t, \mathbf{x}_0)^\top \mathbf{\Phi}(t, \mathbf{x}_0) \mathbf{\Lambda}(t, \mathbf{x}_0), \quad (5)$$

where $\mathbf{\Phi} := \text{diag}(\phi)$ and $\mathbf{\Lambda} := \mathbf{A}^\top(\mathbf{y} - \mathbf{A}\phi)$. Because any solution $\phi(t, \mathbf{x}_0)$ with initial value $\mathbf{x}_0 \in \mathbb{R}_{++}^J$ is in \mathbb{R}_{++}^J for all $t \in \mathbb{R}_+$, the derivative is negative semidefinite for all $t \in \mathbb{R}_+$ and any $\mathbf{x}_0 \in \mathbb{R}_{++}^J$. \square

4. Examples

To illustrate the theoretical result, let us take three examples.

4.1. Example 1

The first one gives an explicit solution to the scalar system. The system (3) with $I = 1$, $J = 1$, $A = a > 0$, and $y > 0$ can be written as

$$\frac{dx}{dt} = ax(y - ax) \quad (6)$$

which, by using separation of variables, can be rewritten as

$$\frac{dx}{ax(y - ax)} = dt.$$

Integrating both sides and using partial fractions, we get

$$\int \frac{dx}{ayx} + \int \frac{dx}{y(y - ax)} = \int dt + c,$$

where c is a constant, and then

$$\frac{1}{ay} \ln|x| - \frac{1}{ay} \ln|y - ax| = t + c,$$

$$\frac{y}{x} - a = Ke^{-ayt}, \quad K = \pm e^{-ayc}.$$

So,

$$x = \frac{y}{a + Ke^{-ayt}}.$$

To find K , let $x(0) = x_0 > 0$. Then we have

$$K = \frac{y}{x_0} - a.$$

Therefore, the solution is

$$\phi(t, x_0) = \frac{y}{a + (\frac{y}{x_0} - a)e^{-ayt}}. \quad (7)$$

We see that $\phi(t, x_0) > 0$ for all $t \geq 0$.

4.2. Example 2

The second example consists of a known phantom image as

$$\mathbf{x}' = \begin{pmatrix} 5 \\ 7 \\ 6 \\ 2 \end{pmatrix}. \quad (8)$$

This simple example is for illustrating behavior of the CIR system, and is made of (2×2) -pixel image and six projection rays with the projection operator and noisy projections, respectively, given by

$$\mathbf{A} = \begin{pmatrix} 1 & 0 & 1 & 0 \\ 0 & 1 & 0 & 1 \\ 1 & 0 & 0 & 1 \\ 0 & 0 & 1 & 1 \\ 1 & 1 & 0 & 0 \\ 0 & 1 & 1 & 0 \end{pmatrix} \quad \text{and} \quad \mathbf{y} = \begin{pmatrix} 14.6891 \\ 5.7118 \\ 5.4928 \\ 5.3800 \\ 14.2761 \\ 10.4708 \end{pmatrix}. \quad (9)$$

Using the least square method, a solution of this example such that the value of $V(\mathbf{x})$ becomes the minimum without constraints is calculated as

$$\mathbf{x}^* = (\mathbf{A}^\top \mathbf{A})^{-1} \mathbf{A}^\top \mathbf{y} = \begin{pmatrix} 7.8922 \\ 5.8926 \\ 5.9332 \\ -1.0445 \end{pmatrix}. \quad (10)$$

It includes a negative value that is physically impossible as a pixel value. We simulated transitions of a solution $\mathbf{x}(t) = (x_1(t), x_2(t), x_3(t), x_4(t))^\top$ starting from the initial state $x_j(0) = 10$, $j = 1, \dots, 4$, in the CIR system described by Eq. (3), as shown in Fig. 1. It was demonstrated that the CIR system does not produce unphysically reconstructed images with a negative pixel value.

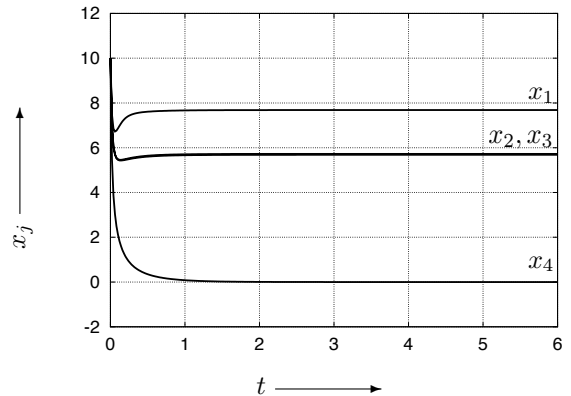


Figure 1: Trajectories for the second example

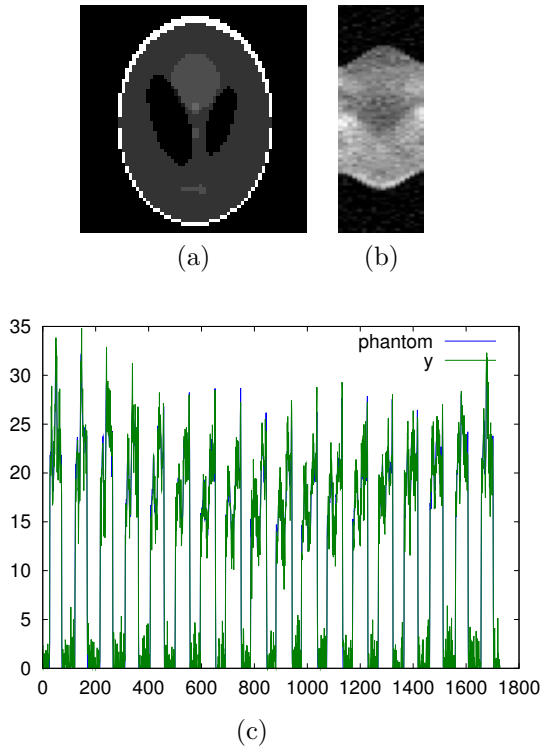
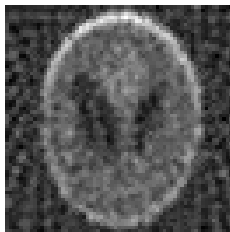


Figure 2: (a) phantom, (b) sinogram, and (c) projections with and without noise



$$D = 25.050$$

Figure 3: Image reconstructed using filtered back-projection

4.3. Example 3

The third example is to deal with an ill-posed image reconstruction problem, assuming the true image with 65×65 pixels ($J = 4225$) and 1728 projection rays ($I = 1728$), which were derived from 96 detectors per projection and 18 projections over 180° scan. The projection data include additive noise generated randomly from a normal distribution. Figures 2 (a), (b) and (c) show the Shepp-Logan phantom image \mathbf{x}' , the sinogram image from the noisy projection \mathbf{y} , and the elements of \mathbf{y} and the noise-free projection \mathbf{Ax}' , respectively. An image obtained from filtered back-

projection (FBP) with a Hanning filter is shown in Fig. 3. The range of the reconstructed pixel values is $[-0.20, 0.78]$, including negative values. Note that D denotes the distance defined by the Euclidean norm between a reconstructed image and the phantom image. Figure 4 shows snapshots of reconstructed images using the linear continuous system in Eq. (4), where D is defined as above. We observe there are artifacts in images obtained from both FBP and the linear continuous methods. While, snapshots of images reconstructed by using the CIR system are illustrated in Fig. 5, where D is defined as above. We obtained reconstructed images gradually deblurred as time proceeds. According to the values of D , the image quality is better than that of other methods.

5. Conclusion

We theoretically verified that the solutions of the CIR system converge to an equilibrium that corresponds to a local minimum of the ill-posed inverse problem. Moreover, we illustrated that the CIR could reconstruct images keeping the non-negativity constraints of pixel values for noisy projection data.

References

- [1] Ken'ichi Fujimoto, Omar M. Abou Al-Ola and Tetsuya Yoshinaga, Continuous-Time Image Reconstruction Using Differential Equations for Computed Tomography (unpublished)
- [2] Ken'ichi Fujimoto, Omar M. Abou Al-Ola and Tetsuya Yoshinaga, Continuous-Time Dynamical System for Reconstructing Computed Tomography Image, IEICE Technical Report, 108 (477) (2009) pp.41–46.
- [3] H. Stark, Image recovery: Theory and applications, Academic, Florida, 1987.
- [4] A. Kak, M. Slaney, Principles of computerized tomographic imaging, IEEE Press, Piscataway, NJ, 1987.
- [5] R. Gordon, R. Bender, G. Herman, Algebraic reconstruction techniques (ART) for three-dimensional electron microscopy and X-ray photography, J. Theor. Biol. 29 (3) (1970) 471–481.
- [6] L. Shepp, Y. Vardi, Maximum likelihood reconstruction for emission tomography, IEEE Trans. Med. Imag. 1 (2) (1982) 113–122.
- [7] H. Hudson, R. Larkin, Accelerated image reconstruction using ordered subsets of projection data, IEEE Trans. Med. Imag. 13 (4) (1994) 601–609.

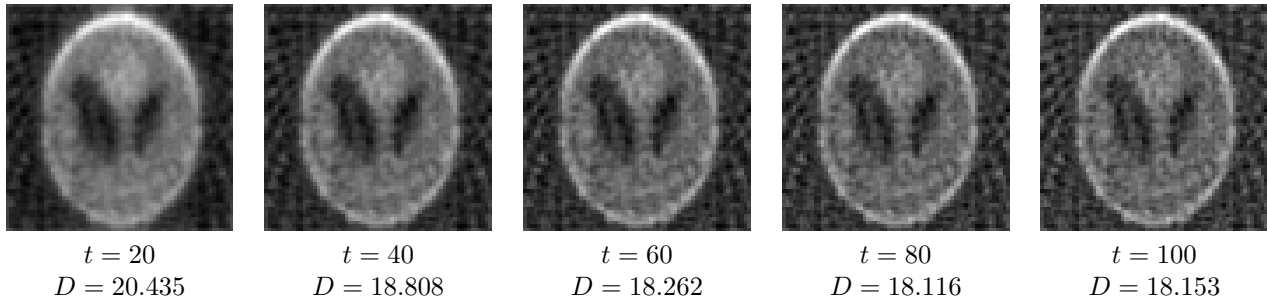


Figure 4: Snapshots of reconstructed images using the linear continuous system

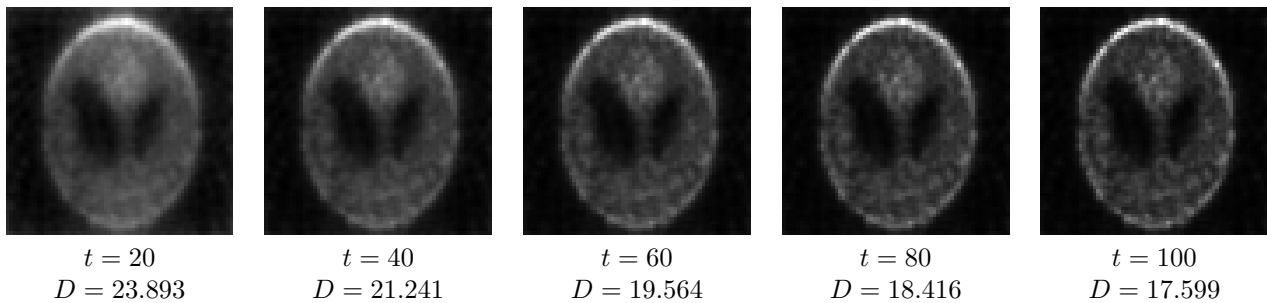


Figure 5: Snapshots of reconstructed images using CIR system

- [8] C. Byrne, Block-iterative methods for image reconstruction from projections, *IEEE Trans. Image Process.* 5 (5) (1996) 792–794.
- [9] J. Schropp, Using dynamical systems methods to solve minimization problems, *Appl. Numer. Math.*, 18 (1995) 321–335.
- [10] R.G. Airapetyan, A.G. Ramm, and A.B. Smirnova, Continuous analog of Gauss-Newton method. *Mathematical Models and Methods in Applied Sciences*, 9 (3), (1999) 463–474.
- [11] R.G. Airapetyan, A.G. Ramm, Dynamical systems and discrete methods for solving nonlinear ill-posed problems, In G.A. Anastassiou, editor, *Applied Mathematics Reviews*, 1, World Sci. Pub. Co., 2000, 491–536.
- [12] R.G. Airapetyan, A.G. Ramm, and A.B. Smirnova, Continuous methods for solving nonlinear ill-posed problems, In A.G. Ramm, P.N. Shivakumar, and A.V. Strauss, editors, *Operator theory and Applications*, volume 25 of *Fields Institute Communications*, American Mathematical Society, 2000, 111–138.
- [13] A.G. Ramm, Dynamical systems method for solving operator equations, *Commun. Nonlinear Sci. Numer. Simul.* 9 (2) (2004) 383–402.
- [14] L. Li and B. Han, A dynamical system method for solving nonlinear ill-posed problems, *Applied Mathematics and Computation*, 197 (2008) 399–406.
- [15] J. Hadamard, *Sur les problèmes aux dérivées partielles et leur signification physique*. Princeton University Bulletin. (1902) 49–52.
- [16] A.G. Ramm, Linear Ill-Posed Problems and Dynamical Systems *Journal of Mathematical Analysis and Applications*, 258 (2001) 448–456.